

# Electrochemical nanogravimetric studies of platinum in acid media

György Inzelt · Balázs B. Berkes · Ákos Kriston · Anna Székely

Received: 11 March 2010 / Revised: 29 March 2010 / Accepted: 30 March 2010 / Published online: 17 April 2010  
© Springer-Verlag 2010

**Abstract** Electrochemical quartz crystal nanobalance (EQCN) is one of the most powerful tools to obtain information on the events occurring at the electrode surface. This method has been exploited to monitor the surface mass changes and hence to draw conclusions in respect of the formation and removal of adsorbed species and oxides as well as changes in the electrochemical double layer also in the case of platinum electrodes. However, the results that had been obtained so far are somewhat contradictory, and consequently diverse interpretations can be found in the literature. Therefore, it is worth to review the knowledge accumulated and to carry out systematic study in this respect. In this work smooth and platinized platinum electrodes in contact with acidic solutions were studied using EQCN technique. The effects of temperature, the nature of cations and anions, pH, concentrations, potential range were investigated on the electrochemical, and the simultaneously detected nanogravimetric responses. It is shown that in the underpotential deposition (upd) of hydrogen the adsorption/desorption of species from the solution phase is governed by the oxidative desorption/reductive adsorption of hydrogen; however, unambiguous conclusions cannot be drawn regarding the actual participation of anions and water molecules in the surface coverage. In the hydrogen evolution region a weak cation adsorption can be assumed and the potential of zero charge can be estimated.  $\text{Cs}^+$  cations affect the EQCN response in the hydrogen upd region. In some cases, e.g., in the case of upd of zinc the mass change can be explained by an

induced anion adsorption. Two types of dissolution processes have been observed. A platinum loss was detected during the reduction of platinum oxide, the extent of which depends on the positive potential limit and the scan rate, and to a lesser extent on the temperature. The platinum dissolution during the electroreduction of oxide is related to the interfacial place exchange of the oxygen and platinum atoms in the oxide region. At elevated temperatures two competitive processes take place at high positive potentials: a dissolution of platinum and platinum oxide formation.

**Keywords** Platinum electrodes · Electrochemical quartz crystal nanobalance · Adsorption · Dissolution

## Introduction

Despite the fact that platinum is among the most thoroughly studied electrode materials [1–4], there is a renewed interest due to the intense fuel cell studies [5–14]. Although many efforts have been spent to replace this precious metal, it is still the mostly used catalyst for both the oxidation of different fuels and also for the oxygen reduction [11–14]. The underpotential deposition (upd) of hydrogen, oxygen, and electrosorption of ions on platinum surface have been investigated by many researchers in the last decades mostly to gain a deeper insight into the relationship between the surface structure and reactivity as well as the nature of the formation of double layer at the metal–electrolyte interface [3–45]. The whole arsenal of surface techniques has also been applied in order to determine the structure of the interphase [4, 6–8, 15–42]. Many studies have been carried out regarding the poisoning of the platinum surface by strong adsorption or chemisorption of different components of the electrolyte or gases which deteriorates the activity of

G. Inzelt (✉) · B. B. Berkes · Á. Kriston · A. Székely  
Department of Physical Chemistry, Institute of Chemistry,  
Eötvös Loránd University,  
1117 Budapest, Pázmány Péter sétány 1/A,  
Hungary  
e-mail: inzeltgy@chem.elte.hu

the catalyst [4, 11–15, 18, 28, 41]. Less attention has been paid to the dissolution and redeposition of the metal which may also cause unwanted effects [7, 11, 14, 43, 44]. Platinum is usually considered as an ideal catalyst which remains unconsumed during the reaction; however, it is not entirely true. It is well known that in media containing chloride or other complexing agents dissolution occurs which results in the formation of chloro or other complexes of platinum [1, 2, 6]. It is surprising, but despite all the efforts even the problem of the nature of the strongly and weakly adsorbed hydrogen has not been solved entirely, yet. There are spectroscopic evidences that the weakly adsorbed form is adsorbed above the Pt plane and so able to interact with the solution. The strongly adsorbed form lying in the plane of platinum surface atoms with its electron in the conduction band of the metal, and therefore it cannot interact with the solution [15]. The diversity of the ideas is partially due to the fact that the behavior of the platinum electrode in the hydrogen upd region strongly depends on the prehistory of the platinum sample, especially the previous oxide formation. For instance, it has been shown that the reduction of hydrous oxide overlaps with the hydrogen adsorption or even the hydrogen evolution regions [19]. Beside the two peaks related to the two forms discussed above, during the anodic scan sometimes a third one also appears between these two peaks. It has been suggested that this peak is due to the oxidation of the sub-surface molecular hydrogen which can form if the Pt surface structure had been disturbed by oxide formation [20]. The results of the radiotracer experiments [3, 4, 39–42] showed that the anion adsorption starts as the adsorbed hydrogen is oxidized not only in chloride-containing solution but also in  $\text{H}_2\text{SO}_4$ . Water adsorption has also been considered simultaneously with or without the adsorption of anions [15, 18, 21, 27, 35–38]. The form of the adsorbed water is still under discussion, beside the weak adsorption of  $\text{H}_2\text{O}$  the dissociative adsorption resulting in  $\text{Pt-OH}^-$  has been suggested, too [21]. In the double layer beside the adsorption of anions and water molecules (or OH species), reorientation of the water molecules and local viscosity effect have also been discussed [23]. The results of the potentiodynamic electrochemical impedance measurements have been interpreted by the variation of the double layer capacitance as a function of the potential even in the double layer region [45].

The electrochemical quartz crystal nanobalance (EQCN) has become a basic tool to study these phenomena [7, 8, 23–38]. The typical EQCN response, that in the majority of the studies on platinum electrodes has been reported, is as follows. A frequency decrease can be detected in the region of the oxidation of adsorbed hydrogen, which continues in the double layer region with a somewhat lesser slope, and a relatively high frequency decrease occurs in the course of

the formation of the oxide layer. While the latter mass increase is obvious, there have been different explanations for the change in the hydrogen region and the double layer region.

In this paper the results of the systematic studies on platinum electrodes in acid media carried out by using EQCN technique are summarized, and the knowledge accumulated concerning the electrochemically induced changes of the surface mass of the platinum electrode are reviewed. A comparison with the results obtained by using other methods provides a deeper understanding of the processes occurring at different potentials. In this work beside the usual basic characterization of platinum electrode in contact with solutions of sulfuric acid of different concentrations and phosphate buffer in the potential range involves the regions of the hydrogen adsorption–desorption and the oxide formation–reduction, the effects of cations, temperature, and the behavior in the hydrogen evolution region, as well as the upd of zinc have been investigated, too. Different and unusual representations have also been used to visualize the effects. The practical consequences have also been emphasized.

### Method, material, and experimental conditions

Five megahertz AT-cut crystals of 1 in. diameter (Stanford Research Systems, SRS, USA) were used in the EQCN measurements. Each side of the crystals was coated with titanium underlayer and platinum. Only one side of the crystals with a projected surface area of  $A=1.22\text{ cm}^2$  was exposed to the electrolyte solution. The piezoelectrically active area was equal to  $0.33\text{ cm}^2$ . The crystals were mounted in the holder made from Kynar and connected to a SRS QCM100 unit. The polished crystals were optically clear, according to the SRS certification their average surface roughness was ca. 5 nm. The roughness factor measured (see below) for smooth virgin crystals was found  $f_r=4\text{--}7$ . After extensive potential scanning involving the oxide region  $f_r$  increased up to ca. 10. The platinized platinum working electrodes were prepared by galvanostatic electrodeposition from a solution of  $0.07\text{ mol dm}^{-3}\text{ H}_2\text{PtCl}_6$  and  $2\text{ mol dm}^{-3}\text{ HCl}$  onto the smooth platinum surface. After the deposition the electrodes were carefully cleaned by rinsing as well as by potential cycling in  $0.5\text{ mol dm}^{-3}\text{ H}_2\text{SO}_4$  solution. In the figure captions the amount of the deposited platinum is indicated ( $1\text{ Hz}=9\text{ ng}$ ). A Pt wire was used as a counter electrode. The reference electrode was a sodium chloride saturated calomel electrode (SCE) that was carefully isolated from the main compartment. The Sauerbrey equation was used for estimation of the surface mass changes ( $\Delta m$ ) from the frequency changes ( $\Delta f$ ), with an integral sensitivity,  $C_f=3.43\times 10^7\text{ Hz cm}^2\text{g}^{-1}$

at 20 °C. The values of the integral sensitivity have been determined by using electrochemical silver deposition/dissolution from solutions containing  $5 \times 10^{-2}$  M AgNO<sub>3</sub> under different conditions (cyclic voltammetry with different scan rates and chronoamperometry at several temperatures), and an average value was used for the calculation of the apparent molar mass value of the adsorbed/desorbed species. An immersion test, i.e., monitoring the frequency decrease after the complete immersion of the crystal from air in water or different solutions of known density and viscosity was also applied to monitor the proper functioning of the crystal, as well as to follow the effect of temperature and surface roughness.

The magnitude of this shift can be calculated by using the following relationship [23, 46]:

$$\Delta f = -f_o^{3/2} \left( \frac{\rho_L \eta_L}{\pi \rho_q \mu_q} \right)^{1/2} \quad (1)$$

where  $\rho_L$  and  $\eta_L$  are the density and viscosity of the liquid contacting one side of the crystal,  $\rho_q = 2.648 \text{ g cm}^{-3}$  and  $\mu_q = 2.947 \times 10^{10} \text{ N m}^{-2}$  are the density and the shear modulus of quartz, respectively.

It was found that the frequency increased logarithmically with temperature which attests that the temperature dependence is mostly due to the change of the viscosity of the solution, and the effect of the variation of density of the solution with temperature can practically be neglected. The variation of the value of the integral sensitivity with temperature was small, less than 1% between 20 and 60 °C, therefore it was neglected. It was also found that while in the case of the smooth electrodes the theoretical frequency decrease occurred after immersion in the solution; however, depending on the extent of platinization (surface roughness) an additional 30–250 Hz frequency decrease was detected. It can be related to the water accumulated in the pores of platinized platinum electrodes. However, because the EQCN responses for platinized platinum electrodes were proportional to the surface roughness values determined, this water content does not play any role, i.e., water molecules do not leave the pores or adsorb in the pores during electrochemical cycling. It makes the comparison of the behavior of electrodes of different surface roughness possible, which is of importance because in most of the previous studies platinized electrodes have been used to increase the frequency response (accuracy) of the measurements.

For the calculation of the apparent molar mass ( $M$ ) of the depositing species the following equation was used:

$$M = \frac{nFA \Delta f}{C_f Q} \quad (2)$$

where  $n$  is the number of electrons transferred in the reaction,  $F$  is Faraday constant,  $A$  is the acoustically active surface area, and  $Q$  is the charge. The measured charge was corrected taking into account the ratio of the piezoelectrically active surface area and the geometric surface area exposed to the solution. It should be mentioned that in the case of platinized platinum electrodes the requirements of the application of the Sauerbrey equation (smooth and uniform surface) [46] is not perfectly met, therefore the proportionality between the frequency response and the true surface area has been checked by using the charges measured in the hydrogen and oxygen upd regions, respectively. The roughness factor ( $f_r$ ) of each electrode was determined from the charge associated with the upd of hydrogen.

Analytical grade chemicals such as H<sub>2</sub>SO<sub>4</sub>, HClO<sub>4</sub>, Na<sub>2</sub>HPO<sub>4</sub>, KH<sub>2</sub>PO<sub>4</sub> (Merck), Cs<sub>2</sub>SO<sub>4</sub> (Sigma-Aldrich), MgSO<sub>4</sub>, and ZnSO<sub>4</sub> (Reanal) were used as received. Doubly distilled water was used. All solutions were purged with oxygen-free argon and an inert gas blanket was maintained throughout the experiments. The three-electrode cell was thermostatted, the temperature was held within  $\pm 0.1$  °C.

An Elektroflex 453 potentiostat (Szeged, Hungary) and a Universal Frequency Counter PM 6685 (Philips) connected with an IBM personal computer were used for the control of the measurements and for the acquisition of the data.

#### General observations

Figure 1a shows a cyclic voltammogram and the simultaneous changes of the surface mass that was calculated from the EQCN frequency response. These are typical responses which have been described in many papers [23, 25, 27, 28, 31, 34–38]. In some works [24, 26, 29] deviations have been observed which were assigned to different reasons, e.g., to the extensive use of the electrode and consequently the changes of the electrode structure; however, the explanations are contradictory, especially when completely opposite EQCN response has been reported [24]. In the course of our rather extensive studies none of these effects have been observed for a well-working electrode. Irregular behavior has been observed only as an experimental artifact, e.g., when the contact between the platinum layer and the quartz became poor.

Therefore, we restrict our discussion to the regular behavior. In Fig. 1b another representation is shown which is instructive regarding the parallelism between the mass change and the charge. It can be seen that the mass changes follow the charge calculated by integration of the cyclic voltammetric curve in both the hydrogen and oxide regions. A deviation can be observed only in the double layer region. Of course, the mass increase in the region of the

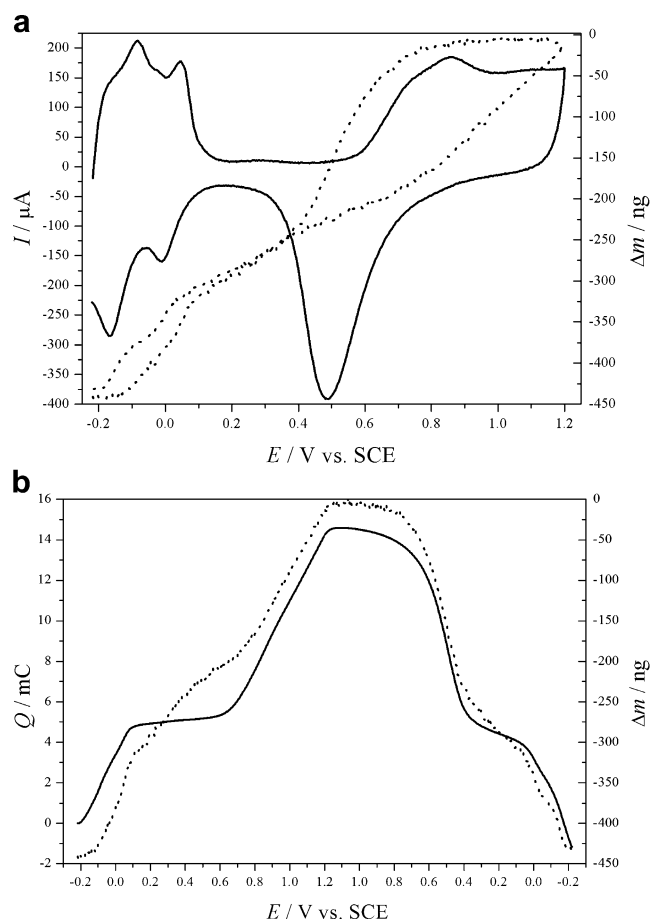


**Fig. 1** The cyclic voltammograms (*continuous lines*) and the simultaneous changes of surface mass ( $\Delta m$ ) derived from the EQCN frequency changes (*dotted lines*; **a**) and the respective charge ( $Q$ ) vs. potential ( $E$ ) (*continuous lines*) and mass change vs.  $E$  curves (*dotted lines*; **b**) for a platinized platinum electrode ( $\Delta f = -1875$  Hz) in contact with  $1 \text{ mol dm}^{-3} \text{ H}_2\text{SO}_4$  at  $20^\circ \text{C}$ . Scan rate,  $10 \text{ mV s}^{-1}$

oxidation of adsorbed hydrogen is still an enigma since mass decrease—albeit a small one due to the low molar mass of hydrogen—could be expected considering the reaction:



The changes are reversible, and during the reductive adsorption mass decrease is detected. We will return the detailed analysis of these changes later.

Usually, nice surface waves for the hydrogen peaks can be obtained, while the oxide formation and reduction peaks show a substantial irreversibility (Fig. 2). In Fig. 2a a slight ohmic shift can also be seen with increasing scan rate which is also due to a resistance effect originating from the increased solution resistance at  $0^\circ \text{C}$ . The shift of the frequency curves into the direction of the higher frequencies followed the order of the experiments (Fig. 2b). The platinum loss (total ca. 90 ng) occurred during the consecutive cathodic cycles—that we will discuss later—practically did not affect the

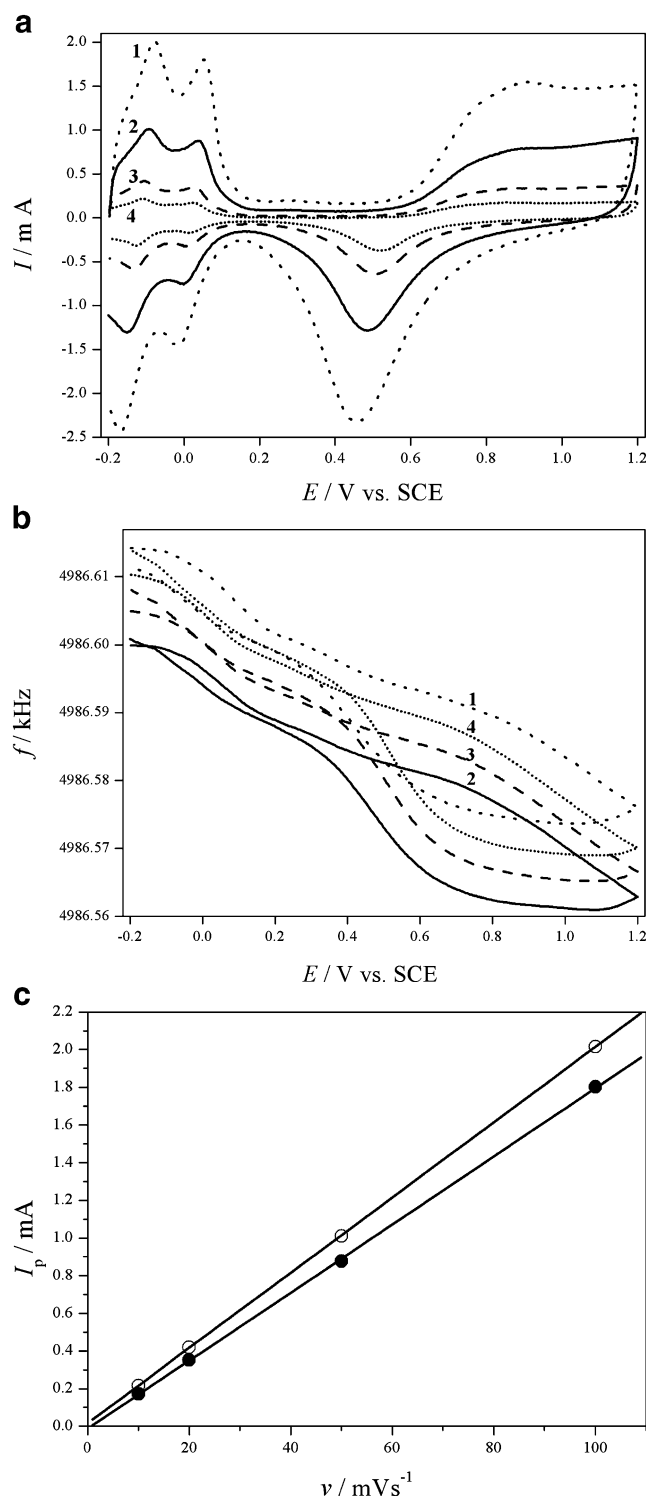


**Fig. 2** Effect of scan rate on the cyclic voltammetric (**a**) and the simultaneously detected EQCN frequency (**b**) responses observed for a platinized platinum ( $\Delta f = -1,950$  Hz) electrode in contact with  $1 \text{ mol dm}^{-3} \text{ H}_2\text{SO}_4$ . Scan rates: (1) 100, (2) 50, (3) 20, and (4)  $10 \text{ mV s}^{-1}$ . The order of the experiments was as follows: (2), (3), (4), and (1). **c** The current vs. scan rate plot for the two hydrogen oxidation waves, first wave (*open circle*) and second wave (*close circle*)

linearity of the peak currents vs. scan rate plots (Fig. 2c). The basic properties of EQCN response practically do not depend on the scan rate; however, the platinum loss during the cathodic half-scan becomes more and more pronounced with decreasing scan rate.

#### The hydrogen region and the double layer region

Figure 3a shows the cyclic voltammogram and the simultaneously obtained changes of the surface mass. The differential curves have also been calculated and displayed in Fig. 3b. The coincidence is certainly striking. It can be stated that the adsorption/desorption of species from the solution phase is governed by the oxidative desorption/reductive adsorption of hydrogen. There are two, diagonally opposite views in the literature. Several authors based on their EQCN investigations have concluded that the mass increase in the region of the oxidation of the adsorbed

hydrogen is mostly or entirely due to the adsorption of water molecules [27, 29, 31, 36–38]. While the direct measurements by radiotracer technique, e.g., by using labeled  $\text{H}_2\text{SO}_4$  in  $\text{HClO}_4$  solution, showed that the amount of adsorbed ions as a function of the potential is rather similar to the mass change—potential curve presented in Fig. 3a, and the curve shown in Fig. 3b resemble the differential voltadiometric curves published in [39–41]. The latter observations clearly attest that there is a direct link between the hydrogen desorption and anion adsorption and vice versa. The phenomenon practically does not depend on the temperature as seen in Fig. 4a where the respective curves were taken at 0 °C by using the same electrode as in Fig. 3. Figure 4b shows the parallelism between the charge consumed and the mass changes derived from the data presented in Fig. 4a.

Regarding the adsorption of ions and also of the water dipoles the charge carried by the electrode is the crucial factor. The value of the potential of zero charge (pzc) of

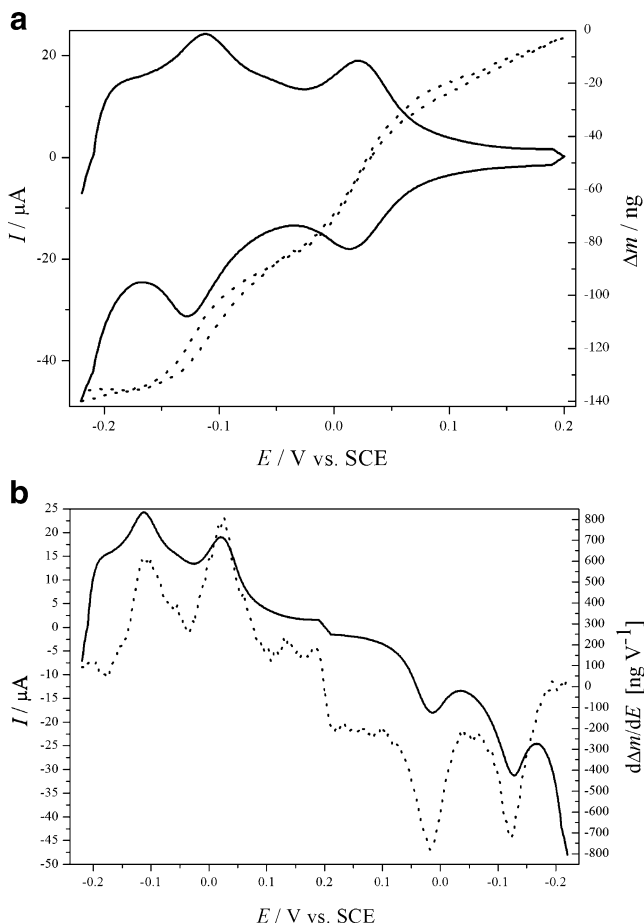


**Fig. 3** The cyclic voltammograms (*continuous lines*) and the simultaneous changes of surface mass ( $\Delta m$ ) derived from the EQCN frequency changes (*dotted lines*) (**a**) and the respective current ( $I$ ) vs. time ( $t$ ; *continuous lines*) and  $d\Delta m/dE$  vs.  $E$  curve (*dotted line*; **b**) for a platinumized platinum electrode ( $\Delta f = -1,950$  Hz) in contact with  $1 \text{ mol dm}^{-3} \text{ H}_2\text{SO}_4$  at 20 °C. Scan rate,  $1 \text{ mV s}^{-1}$

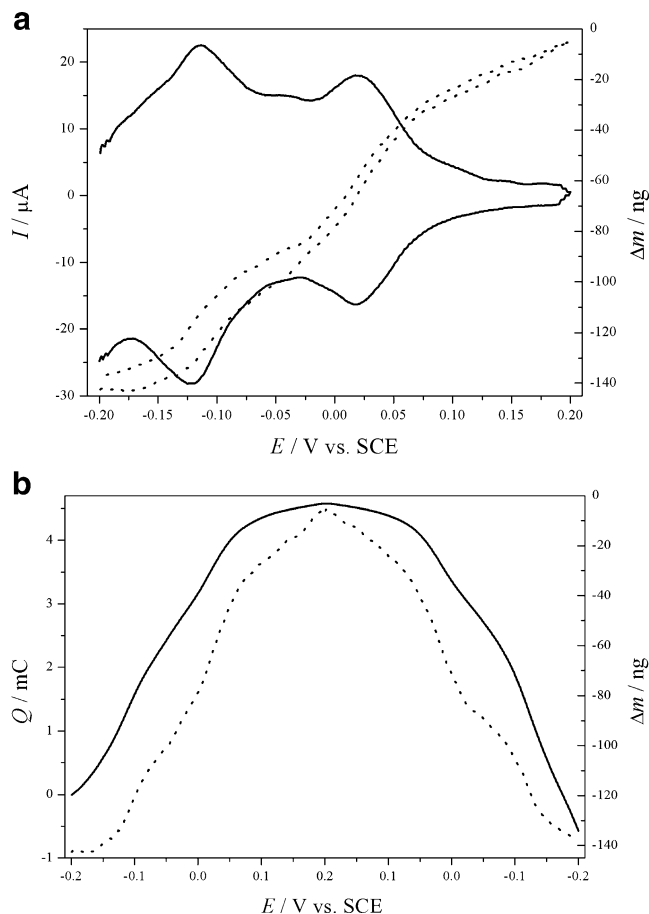


**Fig. 4** The cyclic voltammograms (*continuous lines*) and the simultaneous changes of surface mass ( $\Delta m$ ) derived from the EQCN frequency changes (*dotted lines*; **a**) and the respective charge ( $Q$ ) vs.  $E$  (*continuous lines*) and mass change vs.  $E$  curves (*dotted lines*; **b**) for the platinumized platinum electrode described in Fig. 3 in contact with  $1 \text{ mol dm}^{-3} \text{ H}_2\text{SO}_4$  at 0 °C. Scan rate,  $1 \text{ mV s}^{-1}$

platinum is not known with great accuracy, and it might depend on the composition (pH) of the solution as well as on state of the surface [2]. It is usually considered that the Pt electrode carries a small negative charge in the underpotential deposition region of hydrogen, and the negative charge becomes larger with increasing pH. In order to gain some information in this respect, measurements have been carried out by using more negative switching or initial potentials. As seen in Fig. 5 the intense evolution of hydrogen did not disturb the EQCN frequency signal, and at both pH 0 and pH 2 a frequency maximum appears close to the beginning of the hydrogen evolution. At more negative potentials the frequency change is much smaller than in the hydrogen up-d region. Unfortunately, in this potential interval the apparent molar mass of the adsorbed species cannot be calculated, because the charge is mostly consumed by the formation of molecular hydrogen which leaves the electrode surface. However, logically either adsorption/desorption of hydrogen and/or cations can be assumed. A comparison of the curves displayed in Figs. 4 and 5 reveals that the frequency maximum is practically

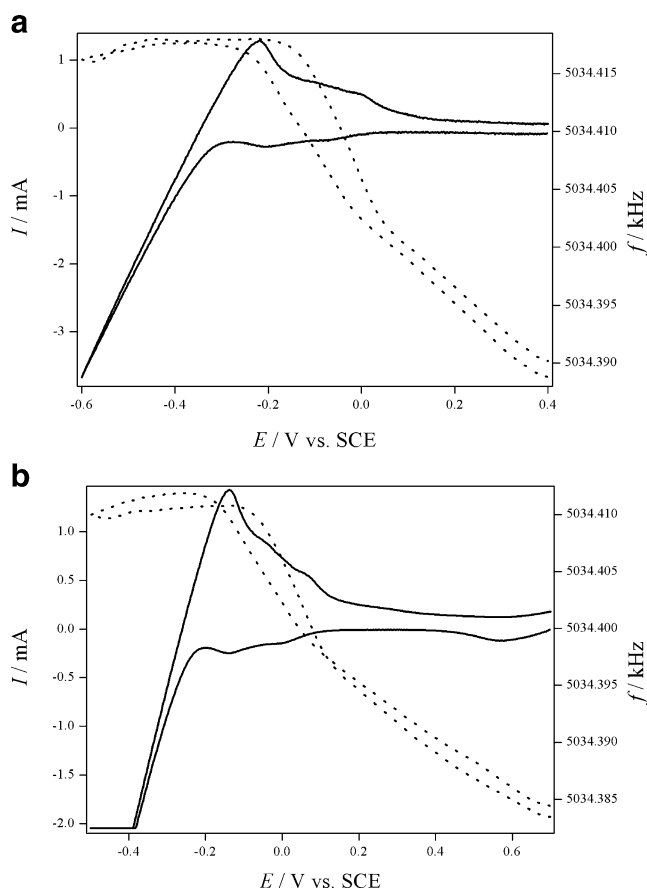


**Fig. 5** The cyclic voltammograms (continuous lines) and the simultaneously obtained EQCN frequency changes (dotted lines) for a platinumized platinum electrode ( $\Delta f = -3,100$  Hz) in contact with  $1 \text{ mol dm}^{-3}$   $\text{H}_2\text{SO}_4\text{-K}_2\text{SO}_4$  solution (pH 2; **a**) and  $1 \text{ mol dm}^{-3}$   $\text{H}_2\text{SO}_4$  (**b**) at  $20^\circ\text{C}$ . Scan rate,  $10 \text{ mV s}^{-1}$

independent of the pH of the solution. According to the radiotracer evidences [42], the potential of zero charge of Pt electrode in the presence of weakly bonded cations such as  $\text{Na}^+$  or  $\text{K}^+$  is unaffected by the changes of pH, and it is equal to  $-0.11 \text{ V vs. SCE}$ . At the pzc both sodium cations and sulfate ions were detected at the surface in equal but small amount. The adsorption of cations increases as the potential becomes more negative while that of the sulfate increases in the direction of more positive potentials. These studies also indicated that the amount of sulfate adsorbed is higher than that of the cations, however, starts to decrease at the beginning of the oxide formation.

The responses obtained at even higher pH but still in acidic solutions (phosphate buffer pH 5.6) essentially do not differ from those detected in lower pH values in sulphuric acid solutions (Fig. 6). Even the replacement of  $\text{HSO}_4^-$  and  $\text{SO}_4^{2-}$  ions by  $\text{H}_2\text{PO}_4^-$  and  $\text{HPO}_4^{2-}$  ions, and the presence of  $\text{Na}^+$  and  $\text{K}^+$  ions does not cause noticeable effect.

It should be mentioned that when the curves obtained at different pH values are displayed in relative hydrogen electrode scale the peaks of the cyclic voltammograms appear at the same potential values.

While the effect of anions have been studied [27, 29, 33, 35–37], less attention has been paid to the effect of cations. It is understandable since specific adsorption of anions is a rather general phenomenon while that of cations (especially alkali ions) is very rare [4]. In this study the effect of the whole series of alkali ions and  $\text{Mg}^{2+}$  ion has been tested. If there were cation adsorption, the highest effect would be expected in the case of  $\text{Cs}^+$  ions and perhaps in the presence of  $\text{Mg}^{2+}$  ions. In the solutions containing different cations mentioned above the behavior of the Pt electrode shows only a minor variation. However, an interesting observation was made in the presence of  $\text{Cs}^+$  ions. While only a rather slight mass increase as a function of potential has been

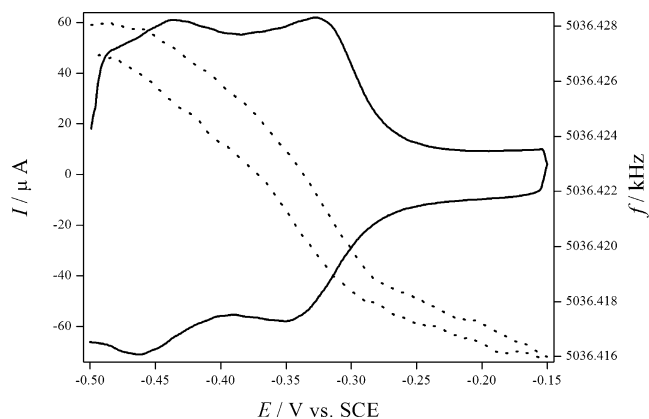


**Fig. 6** The cyclic voltammogram (continuous lines) and the simultaneously obtained EQCN frequency changes (dotted lines) for a platinumized platinum electrode in contact with a solution containing  $0.5 \text{ mol dm}^{-3}$   $\text{KH}_2\text{PO}_4$  and  $\text{Na}_2\text{HPO}_4$  (pH 5.6) at  $20^\circ\text{C}$ . Scan rate,  $5 \text{ mV s}^{-1}$ .  $\Delta f = -1,000$  Hz

observed in the region of the hydrogen evolution in the solution of comparable concentration of  $\text{H}^+$  and  $\text{Cs}^+$  ions as seen in Figs. 7 and 8, rather surprisingly the presence of  $\text{Cs}^+$  ions strongly influenced the EQCN response in the hydrogen upd and the double layer region. (It should be mentioned that until the concentration of  $\text{H}^+$  ions are substantially higher than that of  $\text{Cs}^+$  ions the usual response can be detected.) The frequency decrease in the hydrogen upd region is larger than in sulfuric acid solutions, while there is practically no change in the double layer region (Figs. 7b and 8). There are radiotracer evidences [42], which indicates a stronger adsorption of caesium ions in comparison of sodium ions which is due to an increase in the bonding strength, therefore caesium can be used as a probe of the structure of the electrical double layer. There is another phenomenon which should be mentioned. By adding  $\text{Cs}^+$  ions to the solution of sulfuric acid even in rather low

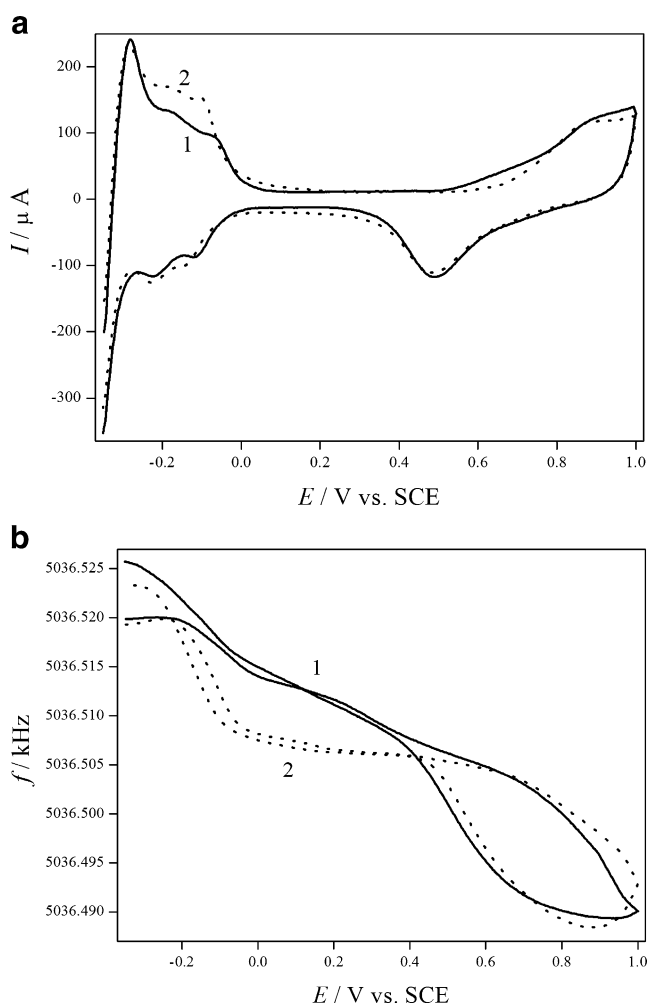


**Fig. 7** The cyclic voltammogram (a) and the simultaneously obtained EQCN frequency changes (b) for a platinumized platinum electrode in contact with a solution containing  $0.05 \text{ mol dm}^{-3} \text{H}_2\text{SO}_4$  (1), and  $0.05 \text{ mol dm}^{-3} \text{H}_2\text{SO}_4$  and  $0.05 \text{ mol dm}^{-3} \text{Cs}_2\text{SO}_4$  (2), respectively, at  $20^\circ\text{C}$ . Scan rate,  $5 \text{ mV s}^{-1}$ .  $\Delta f = -1,000 \text{ Hz}$

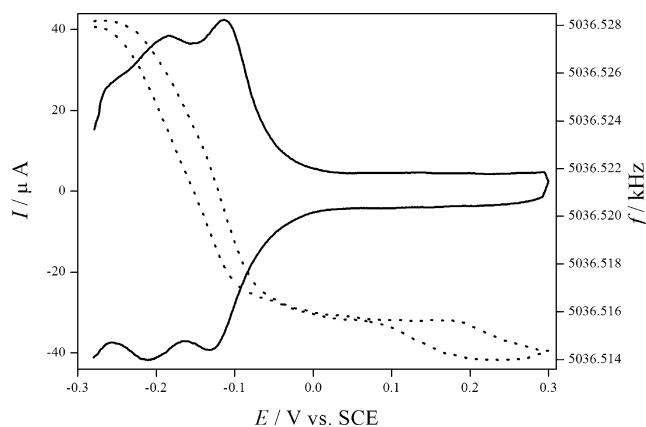


**Fig. 8** The cyclic voltammogram (continuous lines) and the simultaneously obtained EQCN frequency changes (dotted lines) for a platinumized platinum electrode in contact with a solution containing  $0.05 \text{ mol dm}^{-3} \text{H}_2\text{SO}_4$  and  $0.05 \text{ mol dm}^{-3} \text{Cs}_2\text{SO}_4$  at  $20^\circ\text{C}$ . Scan rate,  $2 \text{ mV s}^{-1}$ .  $\Delta f = -1,000 \text{ Hz}$

concentrations always a frequency decrease (5–40 Hz) was observed in the hydrogen evolution, the hydrogen upd, and the double layer regions, which was higher than that could have been expected by the changes of density and viscosity alone. In the oxide layer this difference diminishes. Consequently, it has to be assumed that a certain amount of  $\text{Cs}^+$  ions were bounded to the electrode surface.

Figure 8 reveals another interesting phenomenon. While the EQCN response is reversible an unexpected hysteresis of the frequency can be observed in the double layer region which has never been observed in the absence of  $\text{Cs}^+$  ions. At present it is difficult to offer any explanation based on these results alone. A codeposition of  $\text{Cs}^+$  and  $\text{HSO}_4^-$  or  $\text{SO}_4^{2-}$  and the removal of  $\text{Cs}^+$  ions from the surface as the potential becomes more positive might explain—at least partially—the effect observed. The other possible interpretation could be the consideration of the changing viscosity near the electrode surface, and the hindrance of the adsorption of water molecules since the bulky  $\text{Cs}^+$  ions have no hydration sphere and may prevent the approach of the water molecules to the electrode surface.

In most papers cyclic voltammetry has been combined with piezoelectric nanogravimetry [24–38]. Chronoamperometry or chronocoulometry are less frequently used, perhaps due to the possible damage of the thin metal layer on quartz. The application of potential step techniques is very useful since unlike cyclic voltammetry in this case the charging current and the respective mass response appear in the beginning after a potential step, only. Figures 9 and 10 display the chronoamperometric and chronocoulometric curves and the respective surface mass changes in the hydrogen upd region. The chronoamperometric response obtained during the oxidation of the adsorbed hydrogen is interesting inasmuch as it resembles to the response when phase formation occurs

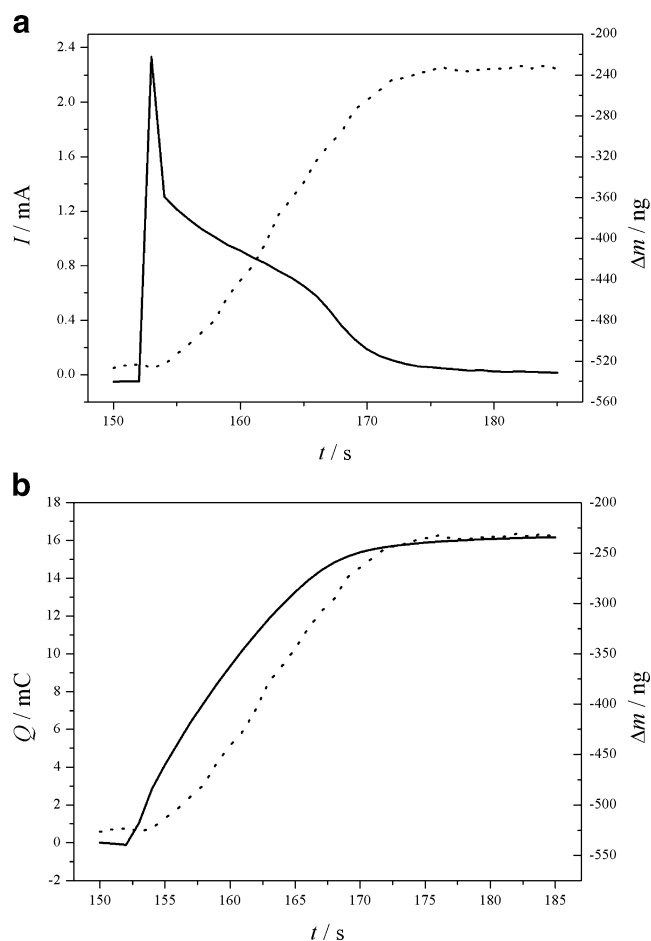


**Fig. 9** EQCN responses of a platinized platinum electrode ( $\Delta f = -3,300$  Hz) by stepping the potential from  $-0.2$  to  $0.4$  V. **a** Current ( $I$ ) vs. time ( $t$ ) and mass change ( $\Delta m$ ) vs.  $t$ , **b** charge ( $Q$ ) vs.  $t$  and  $\Delta m$  vs.  $t$ , functions. Electrolyte,  $1 \text{ mol dm}^{-3} \text{ H}_2\text{SO}_4$ . Temperature,  $50^\circ \text{C}$

(Fig. 9a). However, herein it is most likely that the effect of pseudocapacitance manifests itself in the current response. It is remarkable that there is no substantial change of mass in the beginning, i.e., the charging of the electrochemical double layer causes a minor EQCN response; however, the mass increases continuously and eventually reaches a saturation value when the current drops to zero. The chronocoulometric response shown in Fig. 9b is an expected one, the charge and the mass change run parallel.

The response during the reduction is regular (Fig. 10). The value of the apparent molar mass of the adsorbed/desorbed species, that was calculated from the slope of the mass change vs. charge consumed plots, was found  $9 \pm 2 \text{ g mol}^{-1}$  for several smooth and platinized platinum electrodes in the temperature range between  $0$  and  $60^\circ \text{C}$  which is smaller than that reported in [27]. In [27], almost exactly the molar mass of water was determined in different acid solutions which is rather surprising considering the proven ion adsorption and the fact that the charge consumed related to the oxidation/reduction of hydrogen while the mass change to the

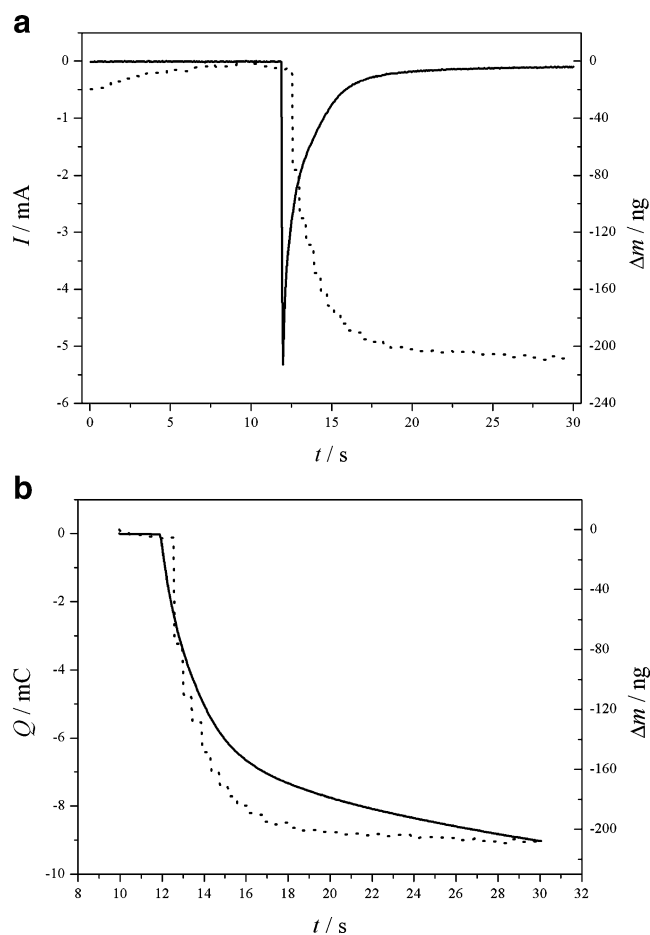


**Fig. 10** EQCN responses of a platinized platinum electrode ( $\Delta f = -3,300$  Hz) by stepping the potential from  $0.25$  V to  $-0.2$  V. **a** Current ( $I$ ) vs. time ( $t$ ), and **b** charge ( $Q$ ) vs.  $t$  and mass change ( $\Delta m$ ) vs.  $t$  functions. Electrolyte,  $1 \text{ mol dm}^{-3} \text{ H}_2\text{SO}_4$ . Temperature,  $60^\circ \text{C}$

desorption/adsorption of a neutral solvent molecule. Considering that the mass change that can be observed during adsorption is always a mass difference of the exchanged species on the surface, and the coverage of the electrode ( $\theta$ ) neither by the anions nor by the solvent molecules reaches a monolayer. In this potential region  $\theta$  is around  $0.1$  for anions, practically any  $M$  value can be reasonable but at the same time useless regarding the establishment of the species attached to the surface. Furthermore, there is a controversy in the literature whether the EQCN is balance or not taking into account the numerous side effects such as viscosity, fluid trapping, slipping, etc. [23, 46].

The oxide region

#### Anodic dissolution of platinum

At elevated temperatures (above ca.  $50^\circ \text{C}$ )—even in the absence of chloride ions or any other complexing agents—especially when the electrode has been extensively used



previously, a dissolution can be observed at about the beginning of the oxide layer formation as seen in Fig. 11. After a frequency decrease in the double layer a frequency increase can be detected that is followed by a frequency decrease again. The frequency maximum observed at ca. 0.8 V vs. SCE at 60 °C is related to competition between platinum dissolution and oxide formation, causing mass decrease and increase, respectively. This frequency change is rather small as compared to the rate of dissolution in the presence of chloride ions. The anodic dissolution of platinum is most likely a  $\text{Pt} \rightarrow \text{Pt}^{2+} + 2\text{e}^-$  reaction [7]. During the cathodic cycle simultaneously with the reduction of the oxide layer a substantial mass loss can be detected. This permanent mass loss is related to three sources. First, to the mass loss due to the removal of oxygen atoms from the surface. Second, to the platinum dissolution during the reduction of the oxide that will be discussed in the next subchapter. Third, to the mass loss related to the active dissolution of platinum at higher potentials, which was dwarfed by the oxide formation in the frequency response, also manifests itself here.

Figure 12 shows the results obtained by stepping the potential from 0.35 to 1.3 V, i.e., from the double layer region to the oxide formation region at 60 °C. The chronoamperometric curve (Fig. 12a) obtained during the oxide formation does not show any special feature. There is a small oscillation of the surface mass in a later phase of the oxidation which is most likely in connection with the oxide formation and the simultaneously occurring dissolution at 1.3 V. From the slope of the mass change ( $\Delta m$ ) vs. charge consumed ( $Q$ ) plot (Fig. 12c) an apparent molar mass value has been calculated. In this case  $M = 17.8 \pm 0.4 \text{ g mol}^{-1}$  was derived by using  $n = 2$ . It can be assigned to the formation of PtO and to the anions adsorbed. Similar  $M$  values have

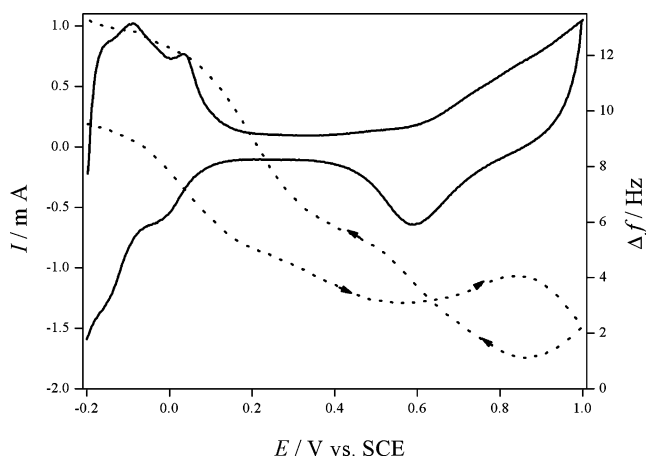


**Fig. 11** The cyclic voltammogram (continuous lines) and the simultaneously obtained EQCN frequency changes (dotted lines) for a platinumized platinum electrode in contact with a solution containing  $0.5 \text{ mol dm}^{-3} \text{ H}_2\text{SO}_4$  at 60 °C. Scan rate,  $20 \text{ mV s}^{-1}$

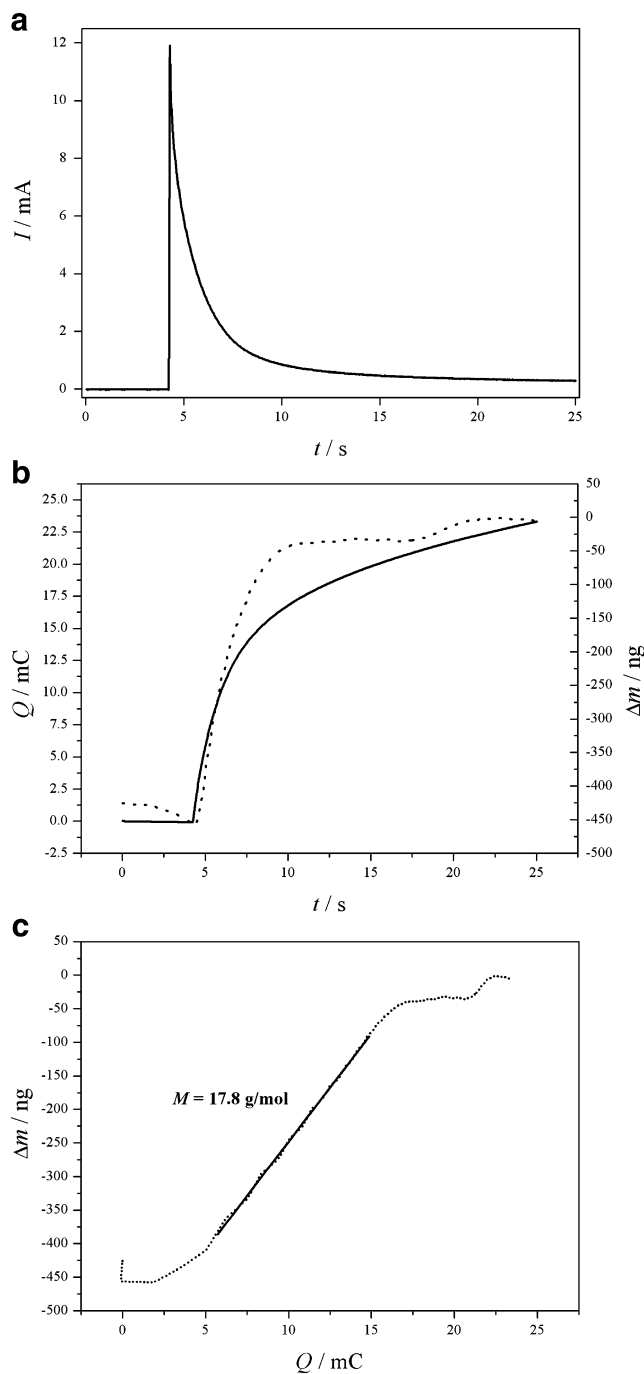


**Fig. 12** EQCN responses by stepping the potential from 0.35 to 1.3 V. **a** Current ( $I$ ) vs. time ( $t$ ), **b** charge ( $Q$ ) vs.  $t$  and mass change ( $\Delta m$ ) vs.  $t$ , and **c**  $\Delta m$  vs.  $Q$  functions. Electrolyte,  $1 \text{ mol dm}^{-3} \text{ H}_2\text{SO}_4$ . Temperature, 60 °C

been reported in [25, 31], and have been interpreted also by the formation of PtO on the surface.

#### Cathodic dissolution of platinum

Figure 13 shows two voltammograms obtained at  $50 \text{ mV s}^{-1}$  with switching potentials of 1.1 and 1.25 V

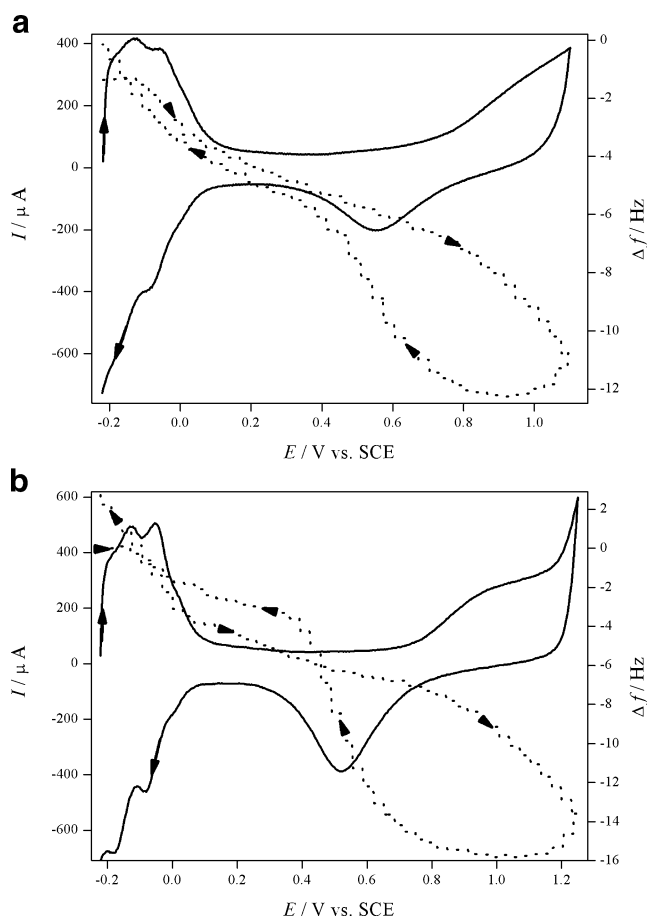


**Fig. 13** The cyclic voltammograms (*continuous lines*) and the simultaneously obtained EQCN frequency changes (*dotted lines*) for a smooth platinum electrode in contact with  $0.5 \text{ mol dm}^{-3} \text{ H}_2\text{SO}_4$  at  $20^\circ\text{C}$ . Scan rate,  $50 \text{ mV s}^{-1}$ . Positive potential limits are **a** 1.1 and **b** 1.25 V vs. SCE.  $\Delta f = f - 4,987,500 \text{ Hz}$

vs. SCE, respectively. When the lower potential limit was used the mass change was reversible (Fig. 13a), however, when the positive potential limit was extended until 1.25 V, after the reduction of the oxide layer a small mass loss was observed (Fig. 13b). With decreasing scan rates the mass loss effect during the cathodic cycle in the same potential region is getting more and more pronounced (Fig. 2).

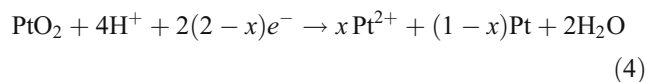
This mass loss is certainly related to the formation and reduction of the oxide layer on the platinum since perfectly reversible response can be detected when cycling is executed only until the end of the double layer region.

The mass loss in the course of a single cycle (9–50 ng) is not too high, however, during consecutive cycling substantial amount of platinum goes into the solution. Considering the theoretical value for a monolayer of platinum ( $1.3 \times 10^{15} \text{ Pt-atom cm}^{-2}$ ) the loss of a complete monolayer would cause ca. 140 ng taking into account the surface area and a roughness factor equal to 1. It follows that ca. 6–35% of the surface platinum atoms will be detached from the surface.

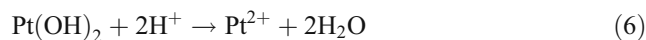
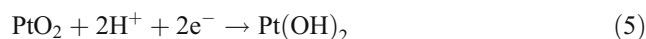
This effect is silent if only the cycling voltammograms are investigated, even an increase in the surface area (roughening) occurs, which is reflected by the higher charge under the peaks due to the oxidative desorption and reductive adsorption of hydrogen as well as the charge related to the oxide formation/reduction. The detachment of platinum atoms (ions or clusters) from the surface during the oxide reduction is of high practical importance. A change of the potential from 0.9–1 V to 0.3–0.4 V of the cathode of a fuel cell frequently happens, e.g., during the acceleration or break when using it in a vehicle. It causes the roughening of the catalyst surface and also dissolution of platinum. The redeposition of platinum particles may occur inside the bulk membrane which leads to a degradation of the performance of the polymer electrolyte membrane fuel cell [14].

Figure 14 shows the results obtained by stepping the potential from 1.3 to 0.35 V, i.e., from the oxide region to the double layer region, at  $60^\circ\text{C}$ .

The responses obtained during the electroreduction of the oxide (Fig. 14) are rather interesting. The current–time response resembles the chronoamperometric curves that can be detected when phase formation occurs. At 1.3 V a small magnitude oscillation of the surface mass can be seen that, as explained previously, is due to the competition between the oxide formation and dissolution. On the other hand, after the potential step the mass change and the charge consumed run parallel. From the linear section of the  $\Delta m$  vs.  $Q$  plot (Fig. 14c)  $M = 20.5 \pm 0.4 \text{ g mol}^{-1}$  was calculated by using  $n = 2$ , which value can be interpreted in terms of the reductive removal of oxygen atoms from the surface as well as the partial desorption of anions adsorbed. From the last phase of the reduction process [from ca.  $-16 \text{ mC}$  (Fig. 14c) or ca. 18 s (Fig. 14a)]  $M = 47.1 \pm 0.4 \text{ g mol}^{-1}$  was derived by using  $n = 2$ . The rather high  $M$  value indicates that beside the oxygen atoms other species were also removed from the electrode surface. There are two reasonable assumptions. Either the platinum atoms (clusters) enter the solution following the reduction of the oxide, provided that a certain number of platinum atoms are not strongly bounded to the underlying Pt atoms due to the place exchange process [15, 16, 31], or platinum ions during the reduction of  $\text{PtO}_2$  formed at 1.3 V according to the following scheme [7, 9, 43]:



or



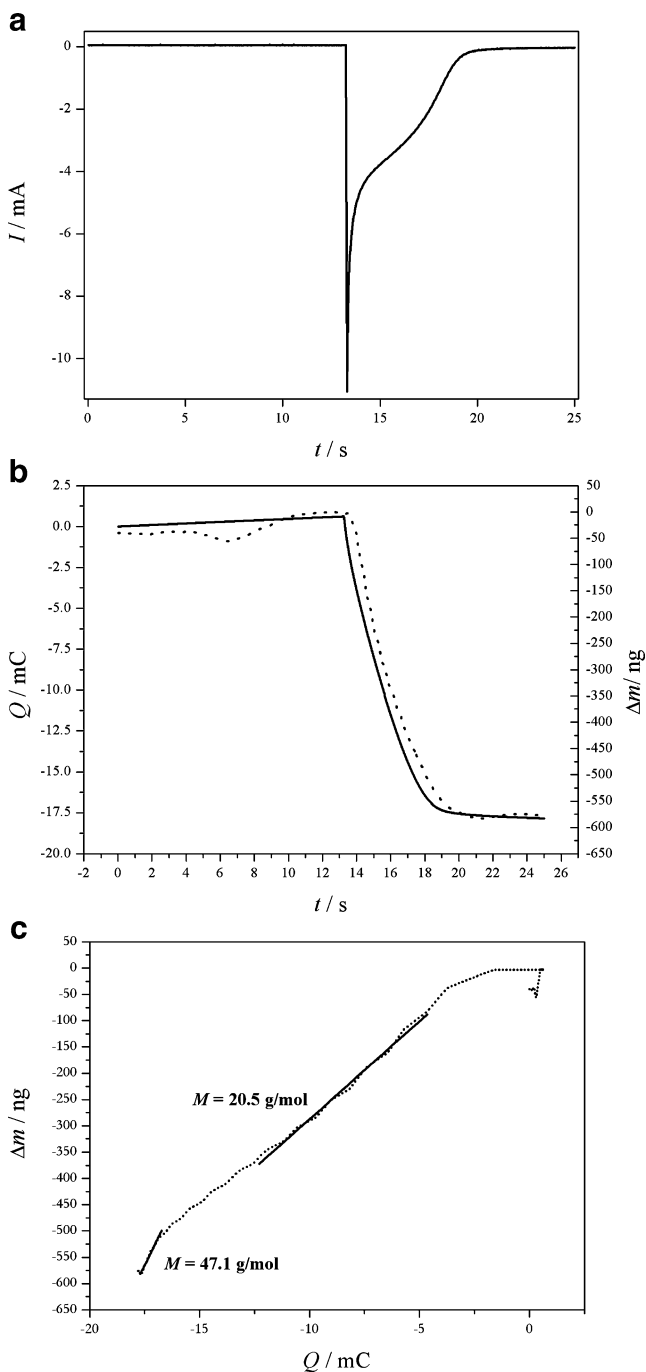


**Fig. 14** EQCN responses by stepping the potential from 1.3 to 0.35 V. **a** Current ( $I$ ) vs. time ( $t$ ), **b** charge ( $Q$ ) vs.  $t$  and mass change ( $\Delta m$ ) vs.  $t$ , and **c**  $\Delta m$  vs.  $Q$  functions. Electrolyte,  $1 \text{ mol dm}^{-3} \text{ H}_2\text{SO}_4$ . Temperature,  $60^\circ \text{C}$

According to the theoretical calculations the detachment of platinum atoms and clusters is an expected process during the reduction of platinum oxides [22]. However, according to our investigations  $\text{Pt}^{2+}$  ions can be found in the solution phase, since the dithizone reaction took place without the reduction by  $\text{SnCl}_2$ . Furthermore, the reductive deposition on an Au electrode at  $-0.2$  V also indicated that the

platinum was present in the form of  $\text{Pt}^{2+}$  ions. The concentration values determined by ICP-MS measurements are well matched with those calculated from the mass loss detected for the Pt electrode by the EQCN.

#### Underpotential deposition and anion adsorption

In several cases the underpotential deposition of metals can be observed. An interesting example is the upd of zinc [47, 48], when the process overlaps with the hydrogen upd as shown in Fig. 15. The mass change observed is much higher than that can be calculated for the monolayer of Zn. Furthermore, in acid solutions zinc adatoms does not perfectly displace hydrogen atoms, a coverage of 0.2–0.7 in respect of zinc has been reported, and it has been demonstrated that by using labeled sulfate species an induced adsorption of anions takes place in the upd region [47, 48]. The mass change observed is in good accordance with values reported on the basis of results of radiotracer experiments.

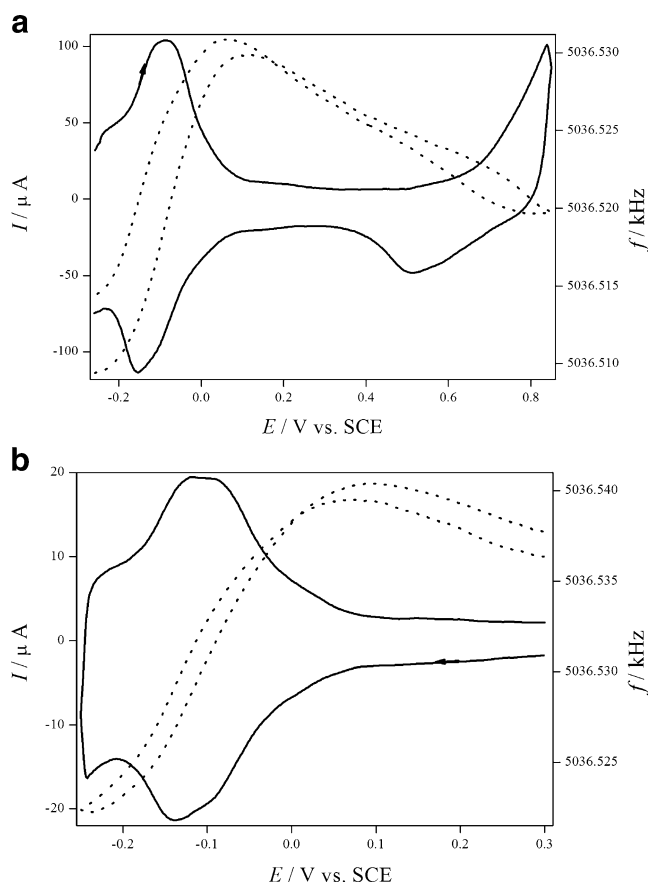


**Fig. 15** The cyclic voltammograms (continuous lines) and the simultaneously obtained EQCN frequency changes (dotted lines) for a smooth platinum electrode in contact with solution of  $0.05 \text{ mol dm}^{-3} \text{ H}_2\text{SO}_4$  and  $0.012 \text{ mol dm}^{-3} \text{ ZnSO}_4$  at  $20^\circ \text{C}$ . Scan rates are  $5 \text{ mV s}^{-1}$  (a) and  $1 \text{ mV s}^{-1}$  (b)

### Factors affecting the EQCN response

The frequency response of the EQCN depends on several factors [23, 46] beside the increase or decrease of the surface mass. Even the mass response can be a function of the elastic or viscoelastic behavior of the deposited material. Several, sometimes interdependent effects have to be considered such as the viscosity and the density of the contacting solution and its possible variation near the electrode surface as a function of potential [23], slippage which may be in connection of the hydrophobic–hydrophilic properties of the surface, surface roughness, temperature, stress, and pressure.

### Effect of surface roughness

In our case the effect of the surface roughness is of utmost interest since in many cases platinized electrodes have been used—in the early studies platinized gold—and consequently the solution occluded between the ridges of a rough surface or in the pores of a porous substrate may substantially affect the response. We have carried out systematic studies by electrodes starting with a smooth one (vacuum-deposited platinum) which has been gradually platinized, and the electrode with different amounts of Pt deposited and surface roughness have been tested after each deposition. It has been found that the frequency change (measured in dry state) was proportional with the amount of the deposited platinum calculated by the charge used for the deposition. The immersion in water of sulfuric acid, phosphoric acid, and phosphates and perchloric acid solutions as well as in acidic solutions containing  $\text{MgSO}_4$  and  $\text{ZnSO}_4$  in the concentration range of 0.01 and 1 M (8 M in the case of sulfuric acid) practically gave the theoretical response calculated from the density and viscosity data [49–51]. The only exception found was observed in  $\text{Cs}^+$  containing solutions when the frequency decrease was somewhat higher than that expected from the viscosity and density variation [50, 51]. The frequency change has been measured in the different potential regions in order to control the state of the surface. The cyclic EQCN responses showed the same characteristics up to a roughness factor,  $f_r \approx 70$ , and the frequency responses were proportional to the roughness factor. The only effect observed was that for electrodes of high roughness factor,  $f_r > \text{ca. } 25$  the immersion into a solution caused a higher than theoretical frequency response by 30–250 Hz; however, the frequency response during a cyclic voltammetric or chronoamperometric perturbation remained proportional to the surface roughness calculated from the hydrogen upd charge, therefore the liquid occluded in the pores did not influence the frequency responses.

An illustrative example is shown in Fig. 16.

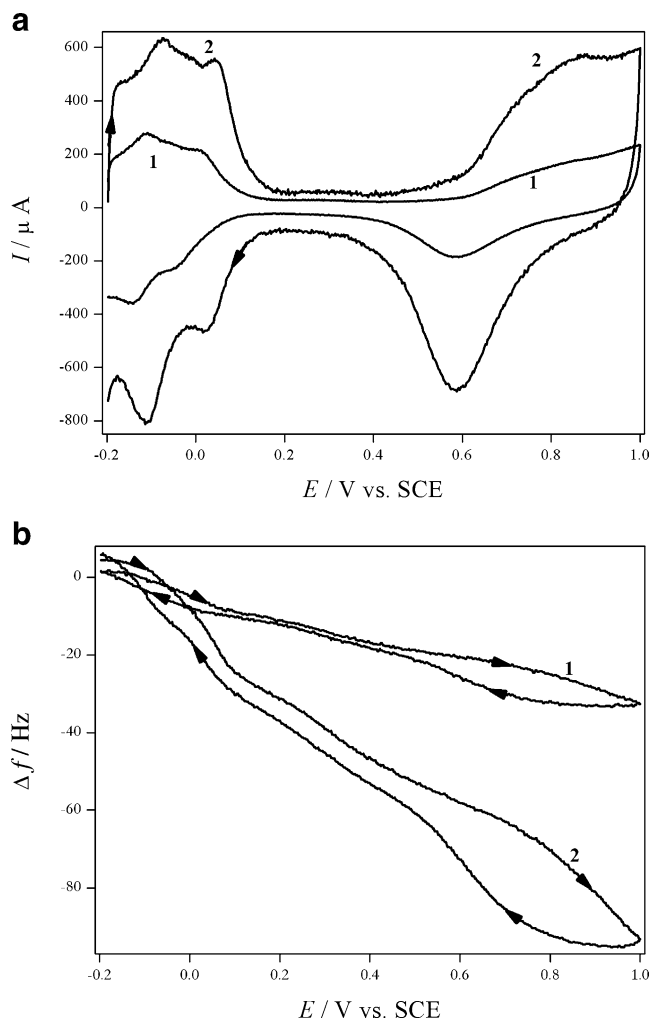


**Fig. 16** The cyclic voltammograms (a) and the simultaneously obtained EQCN frequency changes (b) for platinized platinum electrodes in contact with  $1 \text{ mol dm}^{-3} \text{ H}_2\text{SO}_4$  at  $20^\circ\text{C}$ . Scan rate,  $10 \text{ mV s}^{-1}$ . Frequency changes due to the platinization were: (1)  $-4,250$ , (2)  $-9,010 \text{ Hz}$ . Roughness factors are (1) 24 and (2) 52.  $\Delta f = f - 4,983,455 \text{ Hz}$  and (2)  $\Delta f = f - 4,978,690 \text{ Hz}$

### Effect of temperature

It is also useful to check whether temperature would cause other effects than that can be expected from the temperature dependence of viscosity and density. In this case usually the viscosity is the dominating factor. Figure 17 shows the cyclic voltammetric EQCN responses. It can be seen that temperature causes a rather minor effect, if any, except that is originated from the temperature dependence of viscosity (Figs. 17b and 18). It is also well seen if the frequency difference is plotted against potential all the curves show the same excursion.

Based on the observations described above, it can be stated that the frequency responses measured are due to the mass change on the electrode surface and the changes of the viscosity and/or the density in the double layer play a minor

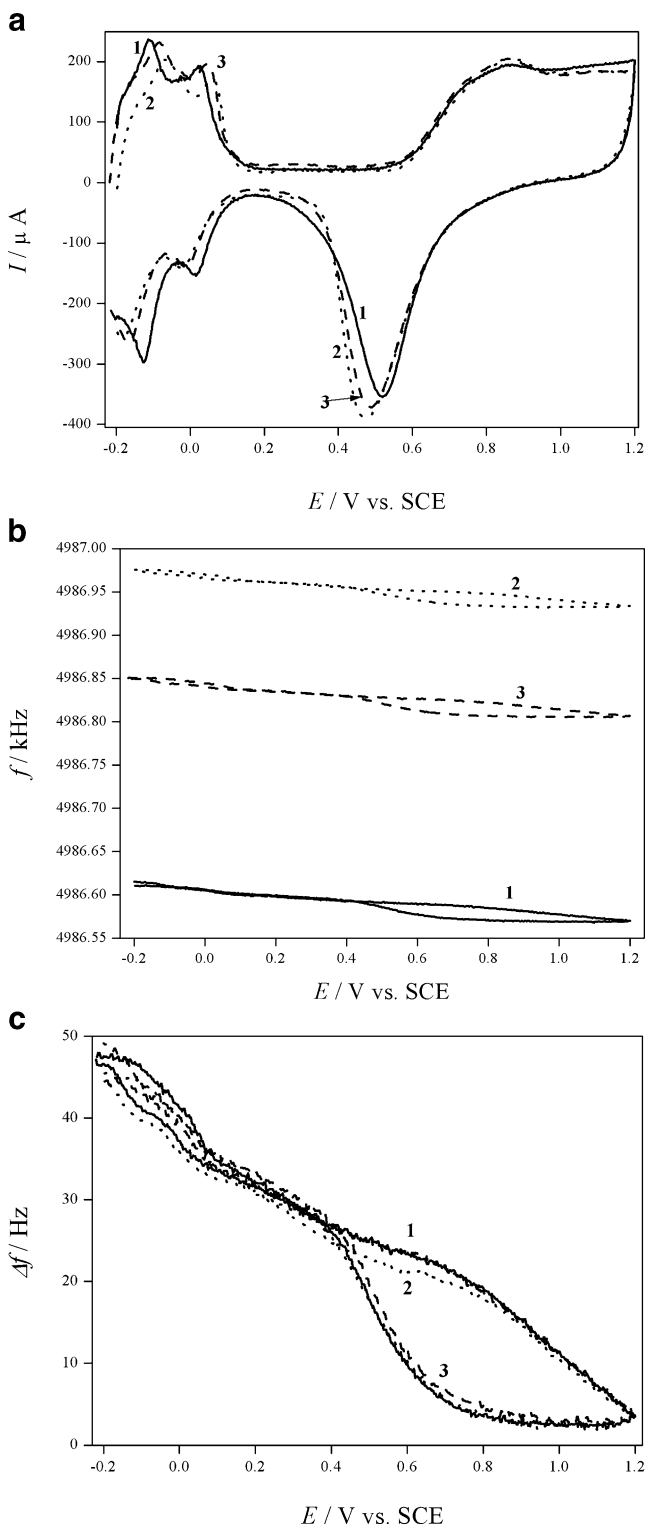


**Fig. 17** The effect of temperature on the cyclic voltammetric (a) and the simultaneously detected EQCN frequency (b) responses at a platinized platinum ( $\Delta f = -1,950$  Hz) electrode in contact with  $1 \text{ mol dm}^{-3}$   $\text{H}_2\text{SO}_4$ . Scan rate,  $10 \text{ mV s}^{-1}$ . Temperatures and the order of cycles are as follows: (1)  $0^\circ\text{C}$  (fourth cycle), (2)  $20^\circ\text{C}$  (13th cycle), and (3)  $40^\circ\text{C}$  (20th cycle). c The respective  $\Delta f$  vs.  $E$  plots

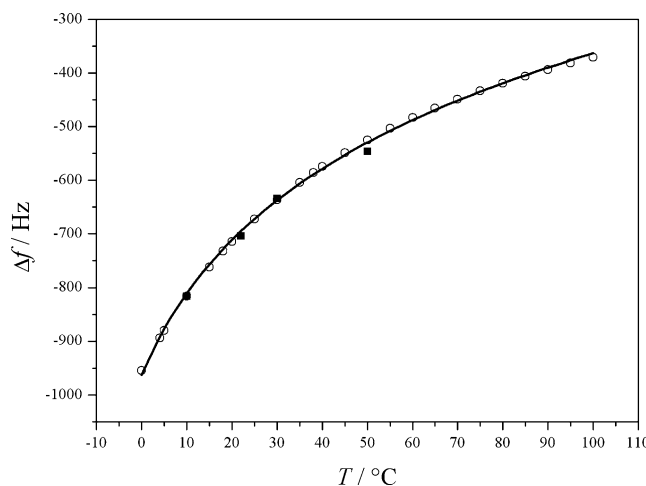


**Fig. 18** The variation of the frequency of a 5 MHz quartz crystal as a function of temperature. Calculated values by using Eq. 1 and the literature data related to the temperature dependence of the viscosity and density of the water (open circle) [49], logarithmic fitting curve (continuous line) and the measured values (close square)

role, only. The accumulation or depletion of ions near the electrode surface due to the charging of the double layer may cause 1–5 Hz frequency change, and this effect should depend on the bulk viscosity and density of the solution. As it has been shown the frequency responses in the double layer region were practically the same by using solutions of a wide range of concentration or varying the temperature, which caused tens of Hz frequency changes due to the viscosity–density effect.

**Conclusions**

Electrochemical quartz crystal nanobalance is a very valuable tool to monitor the adsorption and desorption processes occurring during the electrochemical transformations of platinum electrodes in acidic media. In the present study a systematic investigation has been carried out by varying the experimental conditions (potential range, scan rate, nature and concentration of electrolytes, temperature, and using smooth and platinized platinum electrodes) and the electrochemical methods (cyclic voltammetry, chronoamperometry, and chronocoulometry) in order to clarify the effects of different parameters. This approach allows drawing reliable conclusions and helps the critical review of the previous results. The main results are summarized as follows.

1. In the beginning of the hydrogen evolution region a very small mass change, usually a small mass increase can be observed. It follows that specific adsorption of cations used in this study ( $\text{Na}^+$ ,  $\text{K}^+$ ,  $\text{Cs}^+$ , and  $\text{Mg}^{2+}$ ) cannot be detected, and as expected there is no anion

- adsorption at this potentials. The adsorption of water molecules—if any—does not change in this region.
- The surface mass starts to increase in the underpotential deposition region of hydrogen, therefore the potential of zero charge can be estimated from the minimum of surface mass. There are diverse views concerning the reason of the mass increase in the hydrogen upd region during the oxidation of the adsorbed forms of hydrogen (weakly and strongly bound hydrogen) and the opposite change during the reductive adsorption of hydrogen. The most reasonable assumption is the adsorption or desorption of both anions (also based on the direct radiotracer evidences) and water molecules whose orientation and bonding may change as the potential becomes more positive than the pzc of the electrode. EQCN alone cannot supply evidence in this respect since the mass change observed can be rationalized in infinite combinations. The apparent molar mass of the attached species cannot be calculated properly since the charge is consumed by the oxidation of hydrogen or the reduction of hydrogen ions. Nevertheless, a close link between the hydrogen desorption and hydrogen adsorption and the mass changes has been demonstrated.
  - The elucidation of the mass changes (mass increase during positive charging and the opposite during the other direction) in the double layer region is even more problematic. Here again the adsorption of anions and water molecules should be considered. The effect of the change of viscosity and/or density of the solution near the surface, which also has been proposed, may play a minor role, if any. Practically the same quartz crystal frequency changes have been observed in different media where the frequency decrease in contact with the liquid phase an order of magnitude higher than that can be expected from the potential dependent variation of density and viscosity due to the accumulation of ions near the interface and which change measured in the double layer region. The similar reasoning is hold for the temperature dependence of the frequency variation. An unusual frequency dependence has been observed in the presence of  $\text{Cs}^+$  ions which might be explained by the specific adsorption of  $\text{Cs}^+$  ions and a decreased water adsorption due to the practically unhydrated nature of these ions.
  - The mass change in oxide layer region is in accordance with the formation of  $\text{PtO}$  on the electrode surface. However, the electroreduction of the  $\text{PtO}$  layer may lead to a Pt loss which effect strongly depends on the positive potential limit and the scan rate. It is most likely that the place exchange process involving Pt and O atoms is responsible for this phenomena. The reduction of oxide results in a partial dissolution of platinum and the formation of  $\text{Pt}^{2+}$  ions, which can be detected in the solution phase.
  - At elevated temperatures or in contact with concentrated sulfuric acid solution an anodic dissolution of the platinum takes place even in the absence of any complexing agent. Both the Pt loss during the reduction of  $\text{PtO}$  and the anodic Pt dissolution at elevated temperatures should be considered when Pt electrode or catalyst is applied.
  - It has also been found that the upd of zinc, which occurs in the hydrogen upd region, causes an induced adsorption of anions.
  - A proportionality in the EQCN responses has been measured for platinized platinum electrodes of different surface roughnesses, therefore the results of the early EQCN investigations, when mostly platinized electrodes were used, can be considered without any reservation, and the use of these electrodes in order to increase the frequency response causes no problem. On the other hand, the unusual behaviors that have been reported in the literature are most likely due to different experimental artifacts.

**Acknowledgments** Financial supports of the National Office of Research and Technology (OMFB-00356/2007 and OM-00121-00123/2008) and National Scientific Research Fund (OTKA K71771) as well as GVOP-3.2.1-2004-040099 are acknowledged.

## References

- Woods R (1976) In: Bard AJ (ed) *Electroanalytical chemistry*, vol 9. Dekker, New York, pp 1–162
- Llopis JF, Colom I (1976) In: Bard AJ (ed) *Encyclopedia of electrochemistry of elements*, vol 6. Dekker, New York, pp 170–219
- Horányi G, Inzelt G (2006) In: Scholz F, Pickett CJ, Bard AJ, Stratmann M (eds) *Encyclopedia of electrochemistry*, vol 7a. Wiley-VCH, Weinheim, pp 497–528
- Horányi G (2002) In: Gileadi E, Urbakh M, Bard AJ, Stratmann M (eds) *Encyclopedia of electrochemistry*, vol 1. Wiley-VCH, Weinheim, pp 349–382
- Lee S-J, Pyun S-I, Lee S-K, Kang S-JL (2008) *Israel J Chem* 48:215
- Mitsushima S, Koizumi Y, Uzuka S, Ota K-I (2008) *Electrochim Acta* 54:455
- Yadav AP, Nishikata A, Tsuru T (2007) *Electrochim Acta* 52:7444
- Dam VAT, de Bruijn FA (2007) *J Electrochem Soc* 154:B494
- Umeda M, Kuwahara Y, Nakazawa A, Inoune M (2009) *J Phys Chem C* 113:15707
- Yadav AP, Nishikata A, Tsuru T (2009) *J Electrochem Soc* 156: C253
- Borup R, Meyers J, Pivovar B, Kim YS, Mukundan R, Garland N, Myers D, Wilson M, Garzon F, Wood D, Zelenay P, More K, Stroh K, Zawodzinski T, Boncella J, McGrath JE, Inaba M, Miyatake K, Hori M, Ota K, Ogumi Z, Miyata S, Nishikata A, Siroma Z, Uchimoto Y, Yasuda K, Kimijima K, Iwashita N (2007) *Chem Rev* 107:3904
- Srinivasan S (2006) *Fuel cells*. Springer, New York
- Meyers JP (2008) *ECS Interface* 17:36

14. Yousfi-Steinera N, Mocotéguya Ph, Candussoc D, Hisselb D (2009) *J Power Sources* 194:130
15. Christensen PA, Hamnett A (1994) *Techniques and mechanisms in electrochemistry*. Blackie Academic Professional, London, pp 228–287
16. Nagy Z, You H (2002) *Electrochim Acta* 47:3037
17. Ren B, Xu X, Li XQ, Cai WB, Tian ZQ (1999) *Surf Sci* 427–428:157
18. Zeng D-M, Jiang Y-X, Zhou Z-Y, Su Z-F, Sun S-G (2010) *Electrochim Acta* 55:2065
19. Burke LD, Ahern AJ (2001) *J Solid State Electrochem* 5:553
20. Frelink T, Visscher W, van Veen JAR (1995) *Electrochim Acta* 40:545
21. Marichev VA (2008) *Electrochem Commun* 10:643
22. Noguchi H, Isimaru T, Okada T, Uosaki K (2009) 216th ECS Meeting, Vienna, Austria, Abs 3060
23. Tsionsky V, Daikhin L, Urbakh M, Giladi E (2004) In: Bard AJ, Rubinstein I (eds) *Electroanalytical chemistry*. Dekker, New York, pp 1–99
24. Schumacher R (1990) *Angew Chem Int Ed Engl* 29:329
25. Birss VI, Chang M, Segal J (1993) *J Electroanal Chem* 35:181
26. Raudonis R, Plausinitis D, Daujotis V (1993) *J Electroanal Chem* 358:351
27. Santos MC, Miwa DW, Machado SAS (2000) *Electrochem Commun* 2:692
28. Sitta E, Santos AL, Nagao R, Varela H (2009) *Electrochim Acta* 55:404
29. Wilde CP, De Cliff SV, Hui KC, Brett DJL (2000) *Electrochim Acta* 45:3649
30. Wilde CP, Zhang M (1992) *J Electroanal Chem* 327:307
31. Jerkiewicz G, Vatankhah G, Lessard J, Soriaga MP, Park Y-S (2004) *Electrochim Acta* 49:1451
32. Tian M, Conway BE (2008) *J Electroanal Chem* 616:45
33. Conway B, Zolfaghari A, Pell WG, Jerkiewicz G (2003) *Electrochim Acta* 48:3775
34. Gollas B, Elliot JM, Barlett PN (2000) *Electrochim Acta* 45:3711
35. Gloaguen F, Léger JM, Lamy C (1999) *J Electroanal Chem* 467:186
36. Visscher W, Gootzen JFE, Cox AP, van Veen JAR (1998) *Electrochim Acta* 43:533
37. Watanabe M, Uchida H, Ikeda N (1995) *J Electroanal Chem* 380:255
38. Shimazu K, Kita H (1992) *J Electroanal Chem* 341:361
39. Horányi G, Rizmayer E (1987) *J Electroanal Chem* 218:337
40. Horányi G, Inzelt G (1978) *J Electroanal Chem* 86:215
41. Horányi G (2004) In: Horányi G (ed) *Radiotracer studies of interfaces*. Elsevier, Amsterdam, pp 39–98
42. Wieckowski A (1990) In: White RE, Bockris JO'M, Conway BE (eds) *Modern aspects of electrochemistry*, vol 21. Plenum, New York, pp 65–119
43. Johnson DR, Napp DT, Bruckenstein S (1970) *Electrochim Acta* 15:1493
44. Kulesza PJ, Lu W, Faulkner LR (1992) *J Electroanal Chem* 336:35
45. Ragoisha GA, Osipovich NP, Bondarenko AS, Zhang J, Kocha S, Iiyama A (2010) *J Solid State Electrochem* 14:531
46. Hepel M (1999) In: Wieckowski A (ed) *Interfacial electrochemistry*. Dekker, New York, pp 599–630
47. Horanyi G, Aramata A (1997) *J Electroanal Chem* 434:204
48. Aramata A, Terui S, Taguchi S, Kawaguchi T, Shimazu K (1996) *Electrochim Acta* 41:761
49. Weast RC (ed) (1977–1978) *Handbook of chemistry and physics* 58th edition, CRC, Cleveland Ohio
50. Timmermans J (1960) *The physico-chemical constants of binary systems in concentrated solutions*, vol 3. Interscience, New York
51. Landolt-Börnstein *Zahlenwerte und Funktionen aus Physik Chemie* (1969) Andrussov L, Schramm B, Schäfer K (eds) Sechste Auflage Band II Teil 5, Springer, Heidelberg New York